AD-A041 088   AEROSPACE CORP EL SEGUNDO CALIF VEHICLE ENGINEERING DIV   F/G 20/4
A NUMERICAL STUDY OF NONLINEAR EFFECTS ON BOUNDARY-LAYER STABIL--ETC(U)
FEB 77   J W MURDOCK   F04701-76-C-0077
UNCLASSIFIED   TR-0077(2550-15)-4   SAMSO-TR-77-47   NL

1 OF 1
AD
A041088

END
DATE
FILMED
8-77

MICROCOPY RESOLUTION TEST CHART

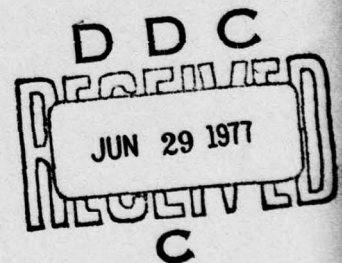NATIONAL BUREAU OF STANDARDS-1963-A

ADA041088

A Numerical Study of Nonlinear Effects on Boundary-Layer Stability

Vehicle Engineering Division
Engineering Science Operations
The Aerospace Corporation
El Segundo, Calif. 90245

28 February 1977

Final Report

D D C
JUN 29 1977
C

Prepared for

AD No.
DDC FILE COPY

This final report was submitted by The Aerospace Corporation, El Segundo, CA 90245, under Contract F04701-76-C-0077 with the Space and Missile Systems Organization, Deputy for Reentry Systems, P.O. Box 92960, Worldway Postal Center, Los Angeles CA 90009. It was reviewed and approved for The Aerospace Corporation by E. C. Hertler, Engineering Science Operations, and J. E. Mullen, Reentry Systems Division. Capt. Edward G. Taylor, SAMSO/RSSE, was the project engineer.

This report has been reviewed by the Information Office (OIS) and is releasable to the National Technical Information Service (NTIS). At NTIS, it will be available to the general public, including foreign nations.

This technical report has been reviewed and is approved for publication. Publication of this report does not constitute Air Force approval of the report's findings or conclusions. It is published only for the exchange and stimulation of ideas.

Edward Taylor, Capt. USAF
Project Engineer

FOR THE COMMANDER

Donald A. Dowler, Col. USAF
Director, Systems Technology
Deputy for Reentry Systems

REPORT DOCUMENTATION PAGE		READ INSTRUCTIONS BEFORE COMPLETING FORM
1. REPORT NUMBER SAMSO-TR-77-47	2. GOVT ACCESSION NO.	3. RECIPIENT'S CATALOG NUMBER
4. TITLE (and Subtitle) A NUMERICAL STUDY OF NONLINEAR EFFECTS ON BOUNDARY-LAYER STABILITY		5. TYPE OF REPORT & PERIOD COVERED Final
		6. PERFORMING ORG. REPORT NUMBER TR-0077(2550-15)-4
7. AUTHOR(s) John W. Murdock		8. CONTRACT OR GRANT NUMBER(s) F04701-76-C-0077
9. PERFORMING ORGANIZATION NAME AND ADDRESS The Aerospace Corporation El Segundo, Calif. 90245		10. PROGRAM ELEMENT, PROJECT, TASK AREA & WORK UNIT NUMBERS 63311F 627A
11. CONTROLLING OFFICE NAME AND ADDRESS Space and Missile Systems Organization Air Force Systems Command Los Angeles, Calif. 90009		12. REPORT DATE 28 February 1977
		13. NUMBER OF PAGES 33
14. MONITORING AGENCY NAME & ADDRESS(if different from Controlling Office)		15. SECURITY CLASS. (of this report) Unclassified
		15a. DECLASSIFICATION/DOWNGRADING SCHEDULE

16. DISTRIBUTION STATEMENT (of this Report)

Approved for public release; distribution unlimited

17. DISTRIBUTION STATEMENT (of the abstract entered in Block 20, if different from Report)

18. SUPPLEMENTARY NOTES

19. KEY WORDS (Continue on reverse side if necessary and identify by block number)

boundary layer
Navier-Stokes equations
Orr-Sommerfeld equation
Blasius solution
stability theory

20. ABSTRACT (Continue on reverse side if necessary and identify by block number)

A spectral scheme is used to solve for the unsteady, two-dimensional flow over a flat plate in the Reynolds number range of transition. Solutions to the full Navier-Stokes equations agree with solutions to the parabolized vorticity equations for the problems considered. The propagation of large amplitude (nonlinear) Tollmien-Schlichting waves in a boundary layer is studied; in some cases, these large amplitude waves are more unstable than linear waves. Analysis of the solutions shows that the relative phase of the first and second harmonics is related to the nonlinear stability of the waves.

DD FORM 1473
(FACSIMILE)

PREFACE

The author wishes to acknowledge the helpful discussions of this work with Drs. T.D. Taylor, P.G. Saffman, and K.J. Victoria.

CONTENTS

FIGURES

1. INTRODUCTION

Boundary-layer transition is a problem of significant engineering importance, which at the present time is not well understood. For design purposes the engineer usually must use empirical correlations of experimental data to characterize transition. One mechanism which leads to transition is the amplification of small disturbances. When the disturbances are infinitesimally small, their behavior is adequately described by linear stability theory, although, as Gaster[1] has shown, there are some ambiguities in applying solutions of the Orr-Sommerfeld equations, which assume parallel flow to nonparallel boundary-layer flows. Nonlinear stability theory extends the linear theory by including the nonlinear terms, but still requires the disturbances to be small. (See Stewartson[2] for a recent review of this subject.) All nonlinear stability analyses known to this author make use of the parallel flow assumption and are valid only in the vicinity of the critical Reynolds number.

Two earlier numerical studies similar to the present work are those of DeSanto and Keller[3] and of Fasel[4,5]. Each of these is a study of boundary-layer stability carried out by integrating the complete two-dimensional,

[1] Gaster, M., "On the Effects of Boundary-Layer Growth on the Flow-Stability," J. Fluid Mech., Vol. 66, 1974, pp. 465-480.

[2] Stewartson, K., "Some Aspects of Nonlinear Stability Theory," Polish Academy of Sciences, Vol. 7, 1975, pp. 101-128.

[3] DeSanto, D. F. and H. B. Keller, "Numerical Studies of Transition from Laminar to Turbulent Flow over a Flat Plate," J. Soc. Indust. Appl. Math., Vol. 10, 1962, pp. 569-595.

[4] Fasel, H., "Numerical Solution of the Unsteady Navier-Stokes Equations for the Investigation of Laminar Boundary Layer Stability," Proceedings of the Fourth International Conference on Numerical Methods in Fluid Dynamics, Springer-Verlag, Berlin, 1974, pp. 151-160.

[5] Fasel, H., "Investigation of the Stability of Boundary Layers by a Finite-Difference Model of the Navier-Stokes Equations," J. Fluid Mech., Vol. 78, 1976, pp. 355-383.

unsteady Navier-Stokes equations. DeSanto and Keller input both small and large amplitude disturbances into the boundary layer and looked at the resultant flow downstream of the disturbance source. Fasel has to date concentrated on small disturbances and thereby investigated the effects of the nonparallel boundary layer on linear stability. (Fasel has indicated in a private communication that he has also carried out large amplitude calculations which are qualitatively similar to the results presented herein.) Solutions to the three-dimensional, unsteady Navier-Stokes equations have been carried out by Orszag[6] and he finds a behavior similar to transition.

The present work is the initial phase of a study whose purpose is to develop a computer code for solving the Navier-Stokes equations (or an appropriate simplified version) in the Reynolds number range of transition and to study the various stages of boundary-layer transition. The nonlinear stability of the Blasius boundary layer is investigated by simulating the physical situation which occurs when a vibrating ribbon introduces disturbances in a boundary layer. The solutions have been obtained by solving both the two-dimensional Navier-Stokes equations and the simpler parabolized vorticity equations. The detailed formulation of these equations is given in Section 2; the spectral method used to solve these equations numerically is described in Section 3.

2.   MATHEMATICAL FORMULATION

Consider the flow of an incompressible fluid over a semi-infinite flat plate. If the flow is assumed to be two-dimensional, then the unsteady Navier-Stokes equations may be written in terms of the vorticity ω and the stream function ψ:

[6]Orszag, S.A., "Turbulence and Transition: A Progress Report," Proceedings of the Fifth International Conference on Numerical Methods in Fluid Dynamics, Springer-Verlag, Berlin, 1976, pp. 32-51.

$$\omega_t + \psi_y \omega_x - \psi_x \omega_y = \nu(\omega_{xx} + \omega_{yy}) \tag{1}$$

$$\omega = \psi_{xx} + \psi_{yy} \tag{2}$$

The independent variables are x, the coordinate parallel to the plate; y, the coordinate normal to the plate; and time t. Equations (1) and (2) will be solved in dimensionless parabolic coordinates, defined by the complex transformation

$$x + iy = x_1 \left[\xi + i\eta \left(2R_{x_1} \right)^{-1/2} \right]^2 \tag{3}$$

where x_1 is a typical distance from the leading edge, and R_{x_1} is the Reynolds number based on the freestream velocity and x_1. The dimensionless time τ is given by

$$\tau = tU_\infty / x_1 \tag{4}$$

The dimensionless dependent variables are defined by

$$\psi = (2\nu U_\infty x_1)^{1/2} \xi f = (2\nu U_\infty x_1)^{1/2} g \tag{5}$$

$$\psi = U_\infty [U_\infty / (2\nu x_1)]^{1/2} \Omega / \xi \tag{6}$$

In terms of these variables, the Navier-Stokes equations are as follows:

$$2\xi \Omega_\tau \left[\eta^2 \Big/ \left(2\xi^2 R_{x_1} \right) + 1 \right] = \Omega_{\eta\eta} / \xi + g_\xi \Omega_\eta / \xi - g_\eta (\Omega/\xi)_\xi + \left[\Omega \Big/ \left(2\xi R_{x_1} \right) \right]_{\xi\xi} \tag{7}$$

$$\xi \Omega \left[\eta^2 \Big/ \left(2\xi^2 R_{x_1} \right) + 1 \right] = g_{\eta\eta} + g_{\xi\xi} \Big/ \left(2 R_{x_1} \right) \tag{8}$$

The term on the left-hand side of Eqs. (7) and (8) containing $R_{x_1}^{-1}$ is negligible compared to unity for $\eta^2 \ll 2\xi^2 R_{x_1}$. Since $\xi^2 = 0(1)$ and $R_{x_1} = 0(10^5)$, the subject term is important only for very large values of η. At large values of η, the vorticity is exponentially small. Therefore, the term in brackets on the left-hand side of Eqs. (7) and (8) may be set to unity with negligible effect on the solution. (A comparison of numerical solutions with the subject terms retained and dropped has confirmed that this term is unimportant.)

Equations (7) and (8) are fourth order in both ξ and η, and consequently require two boundary conditions on each boundary of the solution domain. Most of the boundary conditions are obvious from physical considerations, but the downstream boundary conditions are difficult and, as will be seen, may complicate the numerics. One way to alleviate this problem is to "parabolize" Eq. (7) in the ξ direction. The most accurate way to do this is to substitute Eq. (8) into Eq. (7) and drop the terms of $O(R_{x_1}^{-2})$. This results in a third-order system in ξ, and Eq. (7) becomes

$$2\xi\Omega_T = \Omega_{\eta\eta}/\xi + g_\xi\Omega_\eta/\xi - g_\eta(\Omega/\xi)_\xi + \left[g_{\eta\eta}\bigg/\left(2\xi^2 R_{x_1}\right)\right]_{\xi\xi} \qquad (9)$$

As stated previously, Eqs. (7) and (8) are the Navier-Stokes equations; Eqs. (8) and (9) will be referred to herein as the parabolized vorticity equations. [Some authors neglect the entire last term in Eq. (7) and term the resulting set the parabolized vorticity equations.]

For infinite Reynolds number and steady flow, the two equation sets may be reduced to the Blasius equation:

$$f_{\eta\eta\eta} + ff_{\eta\eta} = 0 \qquad (10)$$

In many cases, the solutions of interest are small relative to the Blasius solution. Thus, to improve numerical accuracy, the inhomogeneous, nonlinear, perturbation equations obtained by subtracting out the Blasius

-8-

solution are actually the ones solved. However, the equations are presented in the usual homogeneous manner to keep the algebra simple and not obscure the physics.

The equation sets will be solved in the semi-infinite region:

$$1 \leq \xi \leq \left(R_{x_2} / R_{x_1} \right)^{1/2} \tag{11}$$

$$0 \leq \eta \leq \infty \tag{12}$$

The boundary conditions at the wall ($\eta = 0$) are such that the two velocity components are zero:

$$g = g_\eta = 0 \tag{13}$$

The station $\eta = \infty$ is upstream of the body in Cartesian coordinates, and the stream function and all its derivatives are known (except for exponentially small terms). The condition on the stream function is

$$g/\xi = f = \eta - \beta \tag{14}$$

where β is a constant characteristic of the displacement thickness. An additional explicit condition on g_η or Ω is not required, as the condition is imposed by the form of the numerical scheme which is discussed in Section 3.

Upstream, at $\xi = 1$, the two velocity components are specified. For the results described subsequently, the upstream boundary condition consists of a linear combination of the Blasius solution and a time periodic solution of the temporal Orr-Sommerfeld equation

$$g = f_{Blasius} + A \, Re \, [\phi(\eta) \exp(-i\omega_r \tau)]$$

$$g_\xi = f_{Blasius} - 2A\alpha \, Im \, [\phi(\eta) \exp(-i\omega_r \tau)] \tag{15}$$

where ϕ is the Orr-Sommerfeld solution for a real wave number α, and ω is the frequency. The imaginary part of ω which causes ϕ to grow or decay in time is ignored and replaced with some fixed amplitude A.

The Navier-Stokes equations require two downstream boundary conditions; the parabolized vorticity equations require only one. Roache[7], in his discussion of outflow boundary conditions used in various finite difference schemes, suggests that conditions on the higher derivatives are less restrictive. The conditions imposed on the Navier-Stokes equations set the first and third normal derivatives of g equal to zero by imposing

$$(\xi\Omega)_\xi = g_\xi = 0 \tag{16}$$

The condition imposed on the parabolized vorticity equations sets the third derivative to zero:

$$g_{\xi\xi\xi} = 0 \tag{17}$$

The ideal downstream boundary conditions have no upstream influence; in steady flow there is no boundary region generated at this boundary, and in unsteady flow there is no upstream reflection of the wavelike disturbances. Unfortunately, the conditions (16) and (17) are not ideal. However, because the calculations are carried out at a very high Reynolds number, the downstream viscous boundary region that occurs when the Navier-Stokes equations are solved is a very small part of the total computation domain, having a thickness Reynolds number on the order of 10. By the same token, the reflected wavelike disturbances which occur for both systems of equations have a limited but larger upstream influence. For the conditions used herein, it was found that the reflected wave decayed to a negligible amplitude in

[7] Roache, P.J., Computational Fluid Dynamics, Hermosa Publishers, Albuquerque, New Mexico, 1972, pp. 154-161.

about a wavelength. (The length Reynolds number of the Orr-Sommerfeld waves used in this study is about 2×10^4.) The main problem with the downstream boundary condition effects is not that they invalidate part of the solution, but that the resulting regions must be resolved or the calculation will be unstable. Thus the boundary region can set the resolution required, and indirectly the time step, and can thereby substantially increase computer storage and running time. The main reason for using the parabolized vorticity equations is that the very thin downstream viscous region is absent, and thus the resolution and time step requirements are not as severe.

Both equation sets are parabolic in time, and the condition imposed at $\tau = 0$ is

$$g = \xi f = \xi f_{Blasius} \tag{18}$$

The Blasius solution has been used as an initial condition because the present study is concerned with perturbations about this solution. Other initial conditions have been used, but none of these solutions is reported here. The Blasius solution, of course, is not an exact solution to either Eqs. (7) and (8) or Eqs. (8) and (9). A solution of either the Navier-Stokes equations or the parabolized vorticity equations with Eq. (13) as the initial condition and no perturbations [A = 0 in Eq. (15)] will produce a correction to the Blasius solution of order $R_{x_1}^{-1}$, consistent with the asymptotic expansion given by Goldstein[8]. These corrections to the Blasius solutions have been generated numerically because this is a convenient problem for testing numerical algorithms. When unsteady perturbations are introduced, they are much larger than $0(R_{x_1}^{-1})$, and thus the resultant solutions are unaffected by the higher order steady part of the solution.

---

[8]Goldstein, S., Lectures on Fluid Mechanics, Interscience, London, 1960, pp. 136-144.

3. NUMERICAL METHOD

The Navier-Stokes equations and the parabolized vorticity equations given in Section 2 have been solved with a "spectral method" (Orszag and Israeli[9]): the dependent variables are expanded in a finite set of orthogonal functions in both space dimensions. This results in a coupled set of ordinary differential equations, with the coefficients of the orthogonal functions as the dependent variables. These equations for the coefficients have been numerically integrated in time with various finite difference methods.

The orthogonal functions are not chosen arbitrarily, but rather must satisfy certain requirements. The following criteria have been used for selecting the orthogonal functions used in this work: (1) the function set should span the same space as the corresponding independent variables; (2) since derivatives are being evaluated, the function set should be such that derivatives of the functions can easily be expressed with the same function set; (3) because the equations are nonlinear, it should be possible to map rapidly the coefficients of the orthogonal functions into a discrete set of physical points, and vice versa; (4) finally, the orthogonal functions should converge rapidly. For the present problem, a form of Chebyshev polynomial is used in both dimensions. For example,

$$\Omega(\xi, \eta, \tau) = \sum_{i=0}^{m} \sum_{j=0}^{n} a_{ij}(\tau) T_i^* \left(\frac{\xi - \xi_1}{\xi_2 - \xi_1} \right) T_j^* \left(e^{-\eta/\eta_r} \right) \tag{19}$$

where T^* is the Chebyshev polynomial defined on the interval zero to one, and η_r is a scale factor. (The properties of Chebyshev polynomials are

---

[9] Orszag, S.A., and M. Israeli, "Numerical Simulation of Viscous Incompressible Flows," Annual Rev. of Fluid Mech., Vol. 6, 1974, pp. 281-318.

given in various books; see, for example, Fox and Parker[10] or Lanczos[11].) The functions used in Eq. (19) are defined on the proper space, and therefore meet the first requirement. The derivatives of polynomials or exponential polynomials are polynomials of the same type, and thus the second requirement is satisfied. An expansion in Chebyshev polynomials, such as Eq. (19), is a Fourier cosine expansion on a distorted physical space. Thus the mapping back and forth between physical space and Fourier space may be carried out using the "fast Fourier transform." (An efficient method for performing cosine transforms with a standard fast Fourier transform routine is given in Cooley, et al.[12].) Orszag[13] has shown that polynomials such as those of Legendre and Chebyshev converge much more rapidly for boundary value problems than periodic functions such as sine and cosine because of the Gibbs' phenomena at the boundary associated with the latter class of functions.

All dependent variables and their derivatives may be expanded in a series of the form (19) except the stream function, which is unbounded at infinity; in this case, the expansion of $g - \eta\xi$, which is finite everywhere, is used. This representation of g together with Eqs. (8) and (14) is sufficient to ensure the desired exponential decay of vorticity at infinity.

[10] Fox, L. and I. B. Parker, Chebyshev Polynomials in Numerical Analysis, Oxford University Press, London, 1968.

[11] Lanczos, C., Tables of Chebyshev Polynomials, U.S. Department of Commerce, National Bureau of Standards, Applied Mathematics Series 9, Washington, D.C., 1952, pp. v-xxvii.

[12] Cooley, J. W., P. A. W. Lewis, and P. D. Welch, "The Fast Fourier Transform Algorithm: Programming Considerations in the Calculation of Sine, Cosine and Laplace Transforms," J. Sound Vib., Vol. 12, 1970, pp. 315-337.

[13] Orszag, S. A., "Numerical Simulation of Incompressible Flows Within Simple Boundaries. I. Galerkin (Spectral) Representations," Studies in Applied Math, Vol. L, 1976, pp. 293-327.

The solutions have been updated in time with both explicit and implicit finite difference methods. The explicit Euler method

$$a_{ij}(\tau + \Delta\tau) - a_{ij}(\tau) = \Delta\tau R_{ij}(\tau) \tag{20}$$

has been used as well as the following, fully implicit method

$$a_{ij}(\tau + \Delta\tau) - a_{ij}(\tau) = 0.5\Delta\tau[R_{ij}(\tau + \Delta\tau) + R_{ij}(\tau)] \tag{21}$$

where a_{ij} are the coefficients of Ω as given in Eq. (19), and R_{ij} denotes the Fourier transform (or coefficients) of the right side of either Eq. (7) or Eq. (9) divided by 2ξ. The evaluation of the linear terms in R_{ij} from the known expansions of g and Ω involves some simple matrix multiplications, the details of which may be obtained from Fox and Parker[10]. The nonlinear terms are obtained by Fourier-inverting the four quantities appearing in the two nonlinear terms, carrying out the indicated multiplications at each discrete point in physical space, and Fourier-transforming the sum of the nonlinear terms. This is an efficient way of evaluating the nonlinear terms, but it does introduce some aliasing error into the result. Orszag and Israeli[9] call this a "pseudospectral approximation" (as opposed to a spectral approximation, in which there is no aliasing error). They suggest that the extra computation time required to remove the aliasing error does not improve the accuracy enough to justify the added computation time; test calculations performed in the preliminary stages of the present work support this conclusion.

Since Eq. (21) is nonlinear, it must be solved by iteration on the quantity $R_{ij}(\tau + \Delta\tau)$. As a first guess, for $a_{ij}(\tau + \Delta\tau)$ the Euler difference equation (20) is used. Subsequent corrections to $a_{ij}(\tau + \Delta\tau)$ are obtained from

$$a_{ij}^{n+1}(\tau + \Delta\tau) - a_{ij}(\tau) = 0.5\Delta\tau[R_{ij}^{n}(\tau + \Delta\tau) + R_{ij}(\tau)] \tag{22}$$

where the superscript denotes the nth level of iteration. When a_{ij}^{n+1} agrees with a_{ij}^{n} to within some specified tolerance, the iteration has converged. Thus, the difference method is in effect a predictor-corrector method, with the number of corrector steps determined by the convergence test. Although the iteration on the implicit difference scheme will converge and is stable for relatively large time steps, the time step which minimizes computer running time is small enough so that convergence is obtained in one to two iterations. For the Navier-Stokes equations, this optimum implicit time step is a factor of four or five greater than the maximum stable explicit time step; for the parabolized vorticity equations, the optimum implicit step is approximately equal to the maximum explicit step. The result is that the implicit method is about twice as fast as the explicit method for the Navier-Stokes equations, and about half as fast for the parabolized vorticity equations. To minimize computer time, the implicit method has been used to solve the Navier-Stokes equations, and the explicit method to solve the parabolized vorticity equations.

Equation (20) or (22), together with the vorticity boundary conditions, completely determines the vorticity (or equivalently its expansion) at the new time or iterate level. However, as is often the case with the vorticity-stream function formulations, some of the vorticity boundary conditions are not known explicitly. In the present case, the two velocity components are specified on the wall and the upstream boundary, resulting in conditions on g and its derivative normal to the boundary.

Two different methods for determining the vorticity boundary conditions have been used. The method which is easiest to implement and which requires the least computer time is an approximate scheme. With this method, the additional boundary conditions are substituted in the Fourier-transformed version of Eq. (8) for the equations governing the highest frequency terms in that dimension. This Poisson-like equation, containing both the Dirichlet and Neumann conditions, gives the new value of the Fourier expansion of g, and the expansion of Ω that satisfies the boundary conditions

-15-

follows from Eq. (8). The more conventional, second method has greater accuracy, but also requires more computation time. Having solved the finite difference equation, one simply guesses the boundary conditions on Ω and solves the Poisson equation for g with Dirichlet conditions. In general, the g so obtained will not satisfy the desired Neumann conditions. The error in the normal derivative of g is then used to correct the boundary value of Ω, and the Poisson equation is solved again. If the corrected Ω is not exact, it may be necessary to iterate this process.

The advantage of the first method of treating the boundary conditions is that all boundary conditions may be imposed simply and the Poisson equation need be solved only once per iteration. The disadvantages of the approach are that numerical instabilities may occur and also that the boundary condition information is somewhat artificially concentrated in the high frequency part of the expansion spectrum. By experimenting with various matrix operators, it was found that the numerical instability problem could be cured by zeroing a column in the second derivative operator (Fourier space operator) for each extra boundary condition in that dimension. The concentration of boundary condition information at high frequencies is controlled if the diffusion is large enough. In the η direction the diffusion is very large, as is obvious from the boundary-layer nature of the flow, and this method of imposing boundary conditions can be used. The situation in the ξ direction is much different; diffusion in this direction is only important on length scale characterized by a Reynolds number of order 10. Using the Chebyshev expansion (which acts very much like a highly variable-mesh finite-difference scheme), it is possible to resolve lengths of this order near the two boundaries, where boundary regions may occur, but not in the center of the computational domain. Thus, in the ξ direction it was necessary to use the second method of imposing the boundary conditions. The method used for obtaining the correct value of the boundary vorticity is described in the following paragraph.

Israeli[14, 15] has considered the problem of finding the vorticity boundary condition at a solid wall when solving the vorticity-stream function equations with a finite difference scheme. He proposed a rapidly convergent iterative scheme for finding the vorticity. This iterative scheme and its convergence properties are based on the fact that the value of the vorticity at a point on the boundary is primarily a function of the normal velocity at that point and a weak function of the normal velocity elsewhere on the boundary. Stated another way, the matrix relation between the vorticity at the grid points on the boundary and the corresponding normal velocities is diagonally dominant. Even though the boundary condition of interest here is at an inflow boundary rather than a wall and the operations are carried out in Fourier space, the situation is much the same. The relation between the Fourier coefficients of Ω and g_ξ at the upstream boundary is diagonally dominant, and a similar iteration will converge rapidly. In the present problem there are usually 17 modes in the η direction [n = 16 in Eq. (19)]; therefore, instead of iterating, the whole matrix is stored (the matrix is actually only 15 x 15 because of the reduction associated with the boundary conditions), and the Poisson equation need only be solved twice per step.

A brief outline of the technique used to solve the Poisson equation will complete the description of the numerical method used to update the solution in time. The inversion of the η operator in Eq. (8) is accomplished using the tensor product method of Lynch, et al.[16]. This requires computing and storing the eigenvalues, the eigenvectors, and the inverse of the eigenvector

[14] Israeli, M., "A Fast Implicit Numerical Method for Time Dependent Viscous Flows," Studies in Applied Math, Vol. LIX, 1970, pp. 327-349.

[15] Israeli, M., "On the Evaluation of Iteration Parameters for the Boundary Vorticity," Studies in Applied Math, Vol. LI, 1972, pp. 67-71.

[16] Lynch, R.E., J.R. Rice, and D.H. Thomas, "Direct Solution of Partial Difference Equations by Tensor Product Methods," Numerische Mathematik, Vol. 6, 1974, pp. 185-199.

array associated with the discrete, Fourier-space, second derivative operator in η. Since only 17 to 21 modes are used in this dimension, the storage requirements are very modest. In the ξ dimension, it is of interest to run rather large problems; for the results described herein, a maximum of 129 modes was used. The inverse in this dimension is carried out by observing that the second integral operator in the ξ dimension is zero, with the exception of the main diagonal and the second diagonal above and below the main diagonal (Fox and Parker[10]). Thus, with some manipulation of Eq. (8), the ξ inversion may be carried out by using an adaptation of the tridiagonal algorithm described in various numerical analysis texts, e.g., Roache[7]. Therefore, the complete inversion of the Poisson equation in the largest case involves two matrix multiplications of arrays sized 17 x 17 and 17 x 129, and 17 solutions of tridiagonal problems involving 129 unknowns.

4.   NUMERICAL RESULTS

The response of the flat plate boundary layer to a periodic disturbance of varying amplitude imposed at $R_x = 10^5$ is described in this section. The disturbance is a solution to the temporal Orr-Sommerfeld equation at $R_x = 10^5$, such that the real part of the complex frequency is

$$\omega_r = \bar{\omega}_r x_1 / U_\infty = 13.16 \tag{23}$$

Most of the computations are carried out in the Reynolds number range $10^5 \leq R_x \leq 2.5 \times 10^5$. The initial condition is the Blasius solution, and at time zero the Orr-Sommerfeld disturbance is turned on at the upstream boundary with a frequency ω_r and an amplitude A. This results in a Tollmien-Schlichting wave being propagated downstream. The calculation is run until the solution is time periodic at all points in the domain. Experience has shown that the solution at a given station is periodic about one period after the disturbance first arrives at that station.

Fasel[4] has published calculations similar to the ones described herein in which small amplitude disturbances are introduced into the boundary layer. It is of interest to compare the neutral stability Reynolds number and the amplitude behavior as a function of Reynolds number computed by Fasel's Navier-Stokes code with the present parabolized vorticity results. At a constant value of y corresponding to $\eta = 58.2/\sqrt{R_x}$ in the present coordinate system, Fasel found that the neutral stability Reynolds number is 1.36×10^5. This is in good agreement with the minimum of the curve shown in Figure 1. At small amplitudes, the disturbance is linear and may be adequately characterized by a dimensionless amplitude ratio as is done by Fasel[4]. To make the comparison in Figure 1, Fasel's dimensionless amplitudes have been scaled such that the "neutral stability point" falls identically on the curve shown. The other points are in good agreement with the curve.

To gain confidence in the validity of the numerical computations when large amplitude disturbances are input into the boundary layer, various self-consistency checks have been made. Figure 2 shows one such comparison in which a Navier-Stokes solution is compared with a parabolized vorticity solution. The agreement in both phase and wave shape is seen to be very good. Both of these calculations were done for a Reynolds number range $10^5 \leq R_x \leq 2.5 \times 10^5$, and 17 modes in the η dimension (n = 16). However, the time step, the ξ resolution, and the time difference method were different. Even though twice as many ξ modes were used in the case of the Navier-Stokes equations, experience suggests this calculation would ultimately be unstable. Because the effective cell Reynolds number at the downstream end of the computation is not 0(1), the viscosity dominated waves reflected off this boundary are not properly dissipated. Instead, these waves propagate back upstream and destroy the whole calculation. The solution region depicted in Figure 2 is free from any influence of reflected waves. If the Navier-Stokes resolution is increased sufficiently, the reflected wave is confined to a finite region near the downstream boundary; the parabolized vorticity equations also admit a reflected wave, but, since the viscous length scale is absent, the requirement for very high resolution is eliminated.
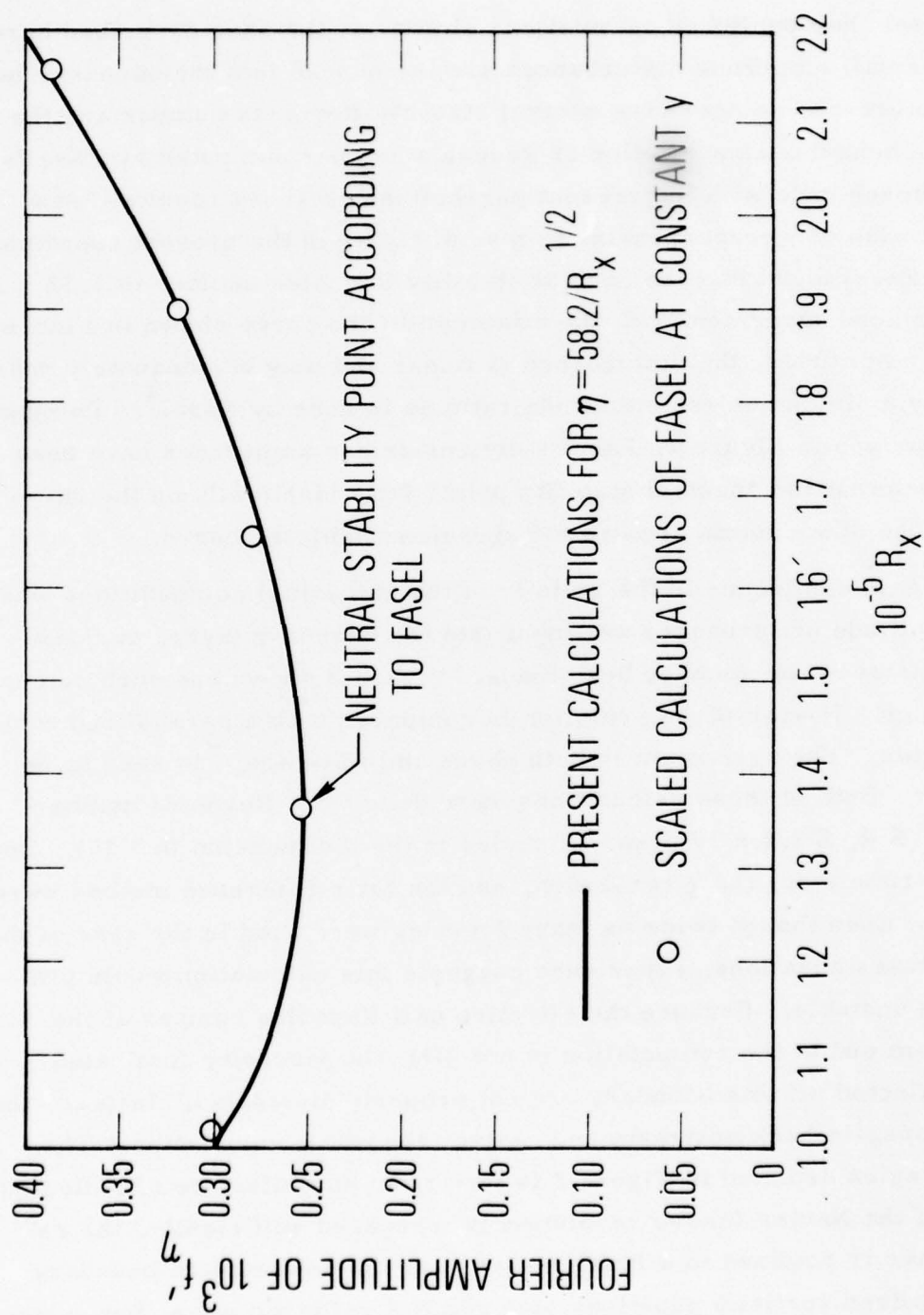
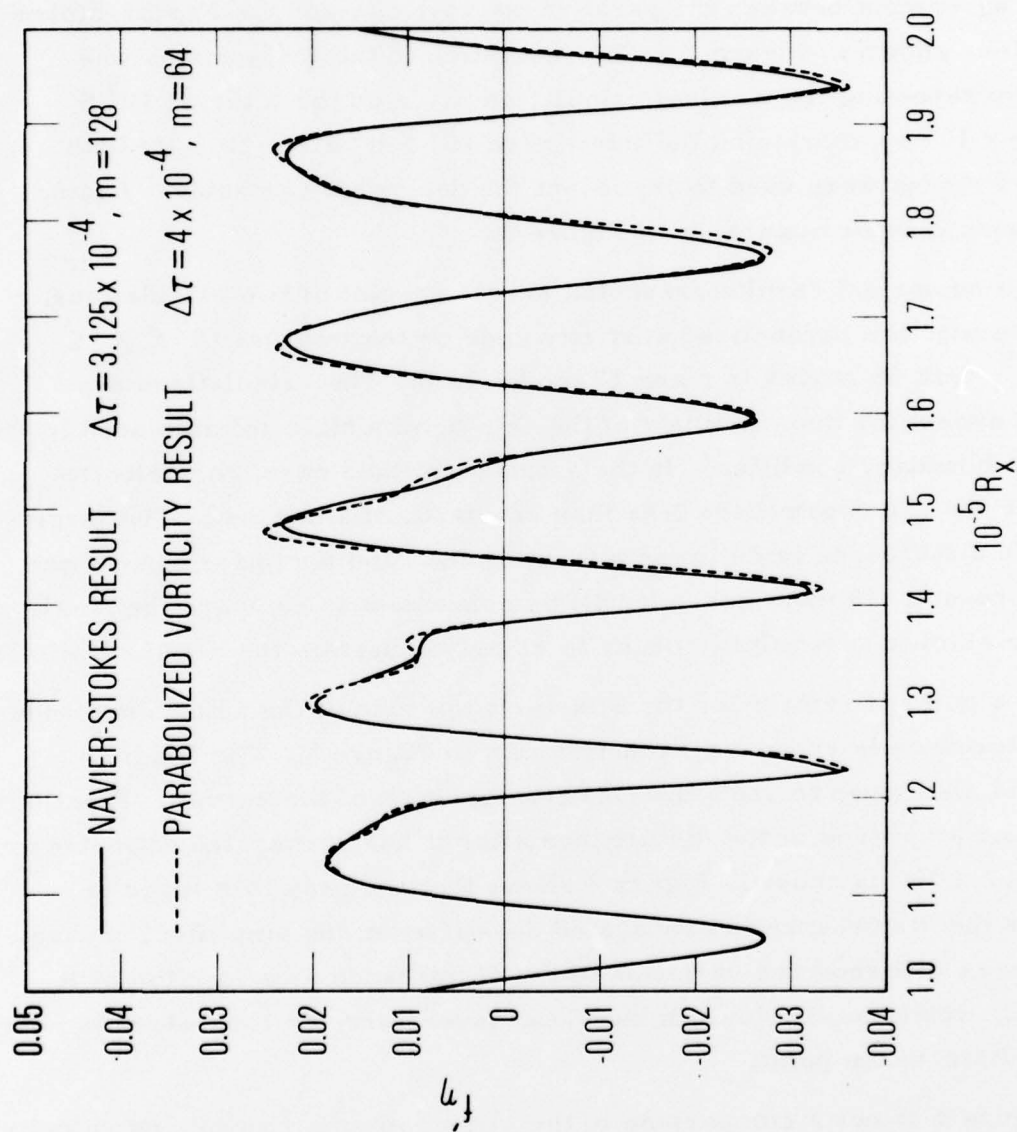Fig. 1. Comparison of Amplitude of u' with
Results of Fasel

The figure shows a plot with the horizontal axis labeled $10^{-5} R_x$ ranging from 1.0 to 2.2, and the vertical axis labeled FOURIER AMPLITUDE OF $10^3 f'_\eta$ ranging from 0 to 0.40. The plot includes:

NEUTRAL STABILITY POINT ACCORDING TO FASEL

$\eta = 58.2/R_x^{1/2}$

Legend:
— PRESENT CALCULATIONS FOR $\eta = 58.2/R_x^{1/2}$
○ SCALED CALCULATIONS OF FASEL AT CONSTANT γ

Fig. 2. Comparison of Navier-Stokes and Parabolized Vorticity Solutions at η 0.2 and τ = 2.75

-21-

To further investigate the validity of the solutions, parabolized vorticity calculations were made in which the resolution in each space dimension was changed. The η resolution was studied by increasing n from 16 to 20. The agreement of the two parabolized vorticity calculations was better than the agreement between the parabolized vorticity and the Navier-Stokes calculations shown in Figure 2. The resolution in the ξ dimension was studied by repeating the nominal calculation made on the interval $10^5 \leq R_x \leq 2.5 \times 10^5$ by shortening the interval to $10^5 \leq R_x \leq 2 \times 10^5$. In both cases, 65 modes were used to represent the dependent variables. Again, the agreement was comparable to Figure 2.

The numerical results presented herein consist of two calculations, both made with the parabolized vorticity code on the interval $10^5 \leq R_x \leq 2.5 \times 10^5$, with 65 modes in ξ and 17 modes in η. The calculations are identical except for the amplitude of the Orr-Sommerfeld solution used in the upstream boundary condition. In the small amplitude case, the velocity perturbations are everywhere less than one-tenth of a percent. The large amplitude disturbance is 80 times the small one, and nonlinear effects are clearly present. In most cases it will be convenient to compare the small and large amplitude results in order to clearly illustrate the nonlinear effects.

As a point of reference, the Fourier amplitude of the small amplitude input disturbance is shown as a function of η in Figure 3. The Blasius solution is also given to show the relative variation of the curves. Finally, the Fourier amplitude of the disturbance after it has propagated downstream to $R_x = 2.2 \times 10^5$ is shown. Figure 3 shows that the peak in η space is shifted as the disturbance is propagated downstream and amplified. Subsequent curves will show the variation of the disturbance as a function of R_x at $\eta = 0.2$, which is well down in the shear layer, and $\eta = 1.0$, which is near the peak disturbance point.

Figure 4 shows a comparison of the large and small amplitude velocity perturbation at the η location inside the shear layer, as a function of R_x. While the small amplitude disturbance closely resembles a modulated
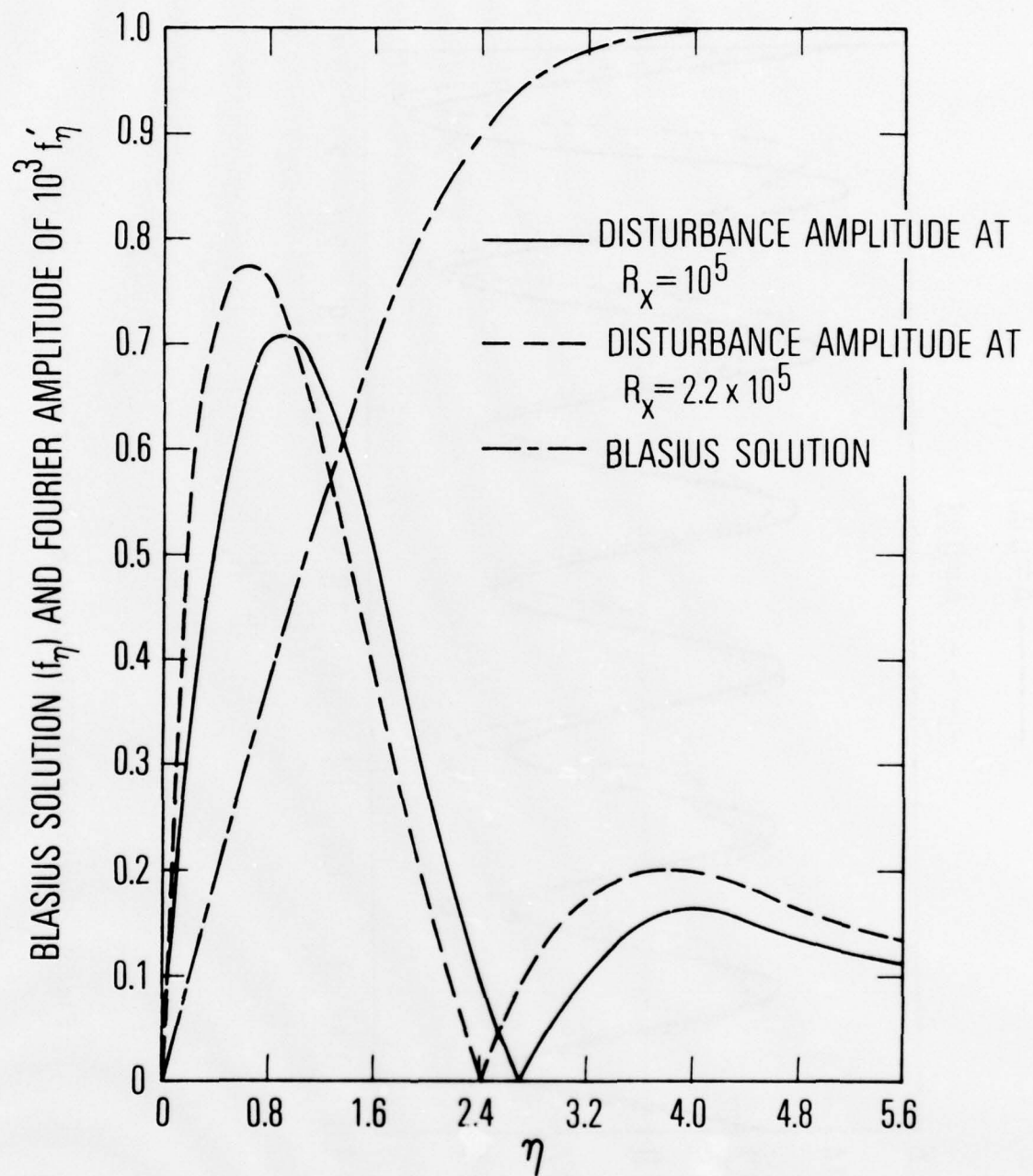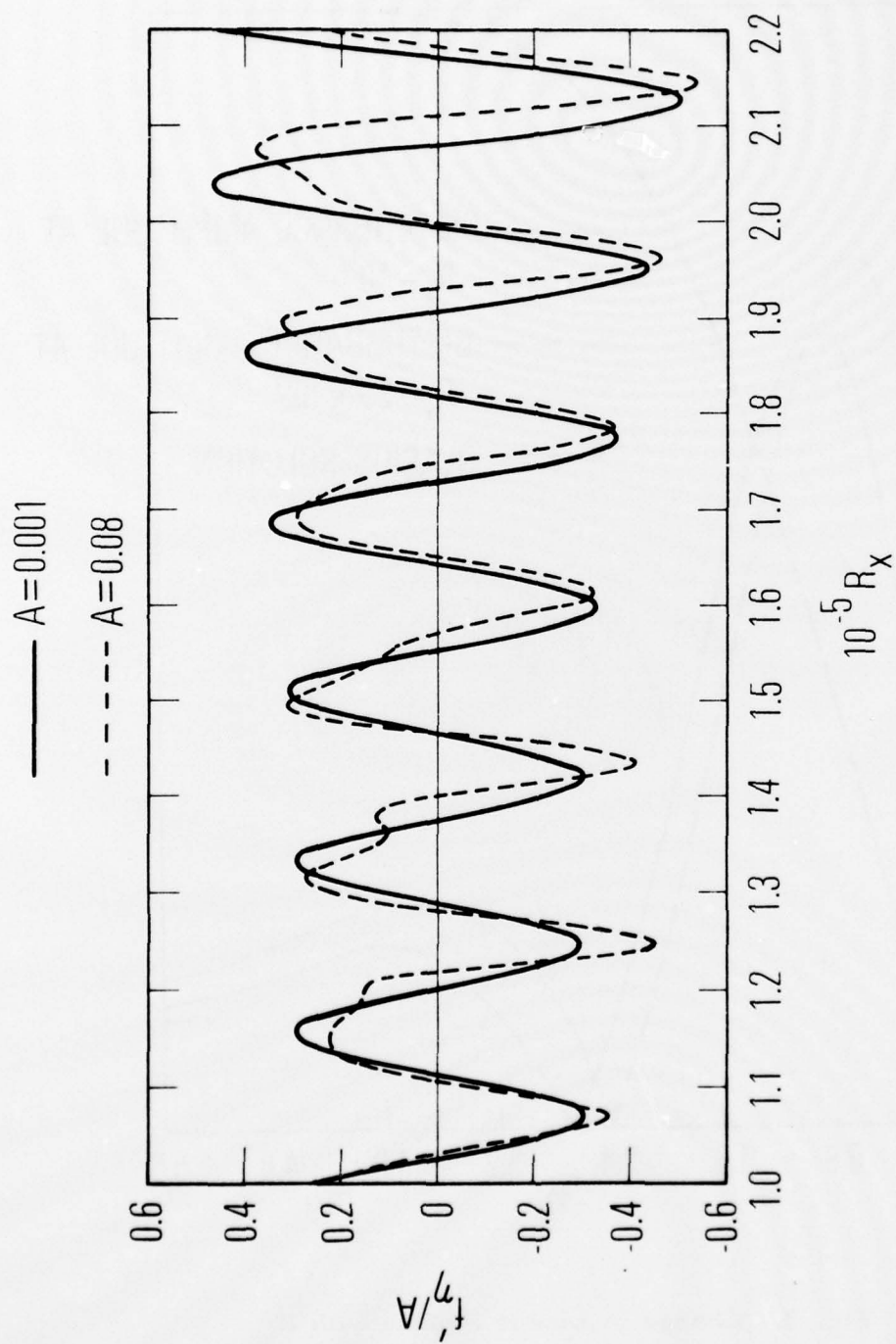
Fig. 3. Change in Linear Profile with R_x

Fig. 4. Perturbation Velocity at $\eta = 0.2$, $\tau = 4.2265$

sinusoid, the large amplitude perturbation is significantly distorted. However, as noted previously, the disturbance at any station is periodic in time with the period of the upstream disturbance. This fact suggests that a Fourier series in time will allow a clearer interpretation of the physics than curves such as those in Figure 4.

The Fourier amplitude of the perturbation velocity is illustrated in Figure 5 at the same station in the boundary layer as Figure 4; the Fourier amplitude at a station near the location of the maximum disturbance is shown in Figure 6. The large amplitude curves (A = 0.08) in Figures 5 and 6 show that up to $R_x = 1.3 \times 10^5$ the primary mode is changed only slightly from the linear behavior, while the second mode grows substantially. Thus in this range, the nonlinear effects which feed energy into the second mode are destabilizing. Beyond the maximum amplitude point of the second mode, the relative stability becomes a matter of definition.

The perturbation velocity is herein defined relative to the Blasius and therefore the mean perturbation is not zero in the large amplitude case. The mean perturbation shown in Figures 5 and 6 is clearly less important than the second harmonic. The higher harmonics are even smaller than the mean and are therefore not shown.

Figures 5 and 6 suggest that the amplitude of the second harmonic relative to the first harmonic is a function of η. Thus, the variation of the harmonic components with η is illustrated at two values of the Reynolds number in Figures 7 and 8. At $R_x = 1.3 \times 10^5$ the large and small amplitude primary mode shapes are very similar. The shape of the secondary is qualitatively similar to that of the primary, but the peak and phase reversal points are closer to the wall. The mean perturbation velocity is positive near the wall with a smaller negative region adjacent. (Only absolute values are shown in the figure.) Figure 8 shows a similar result at $R_x = 2.2 \times 10^5$. At this Reynolds number, the primary disturbances are different for the two values of A. The mean contribution again has a positive region near the wall, followed by a now significant negative region.
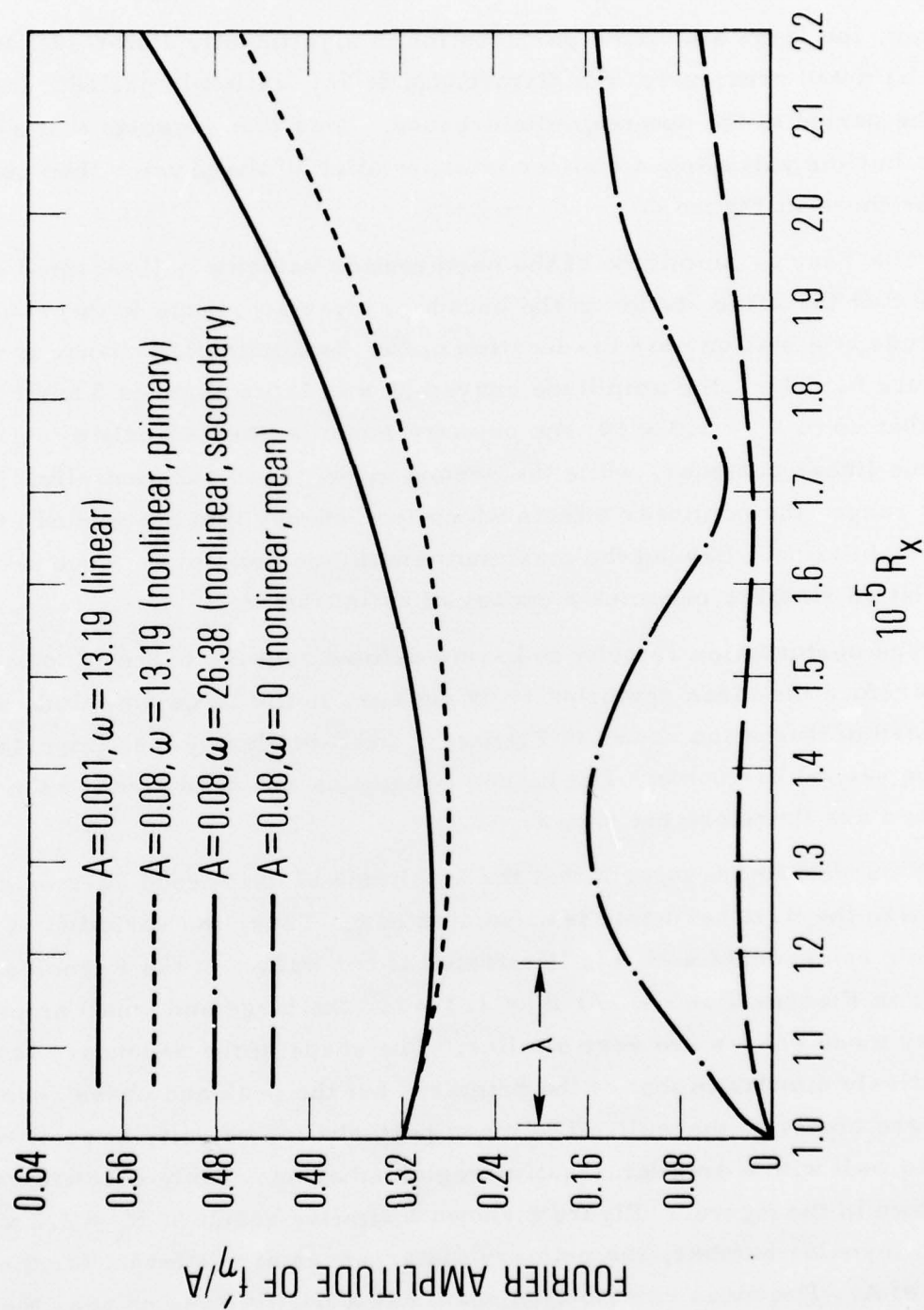
-25-

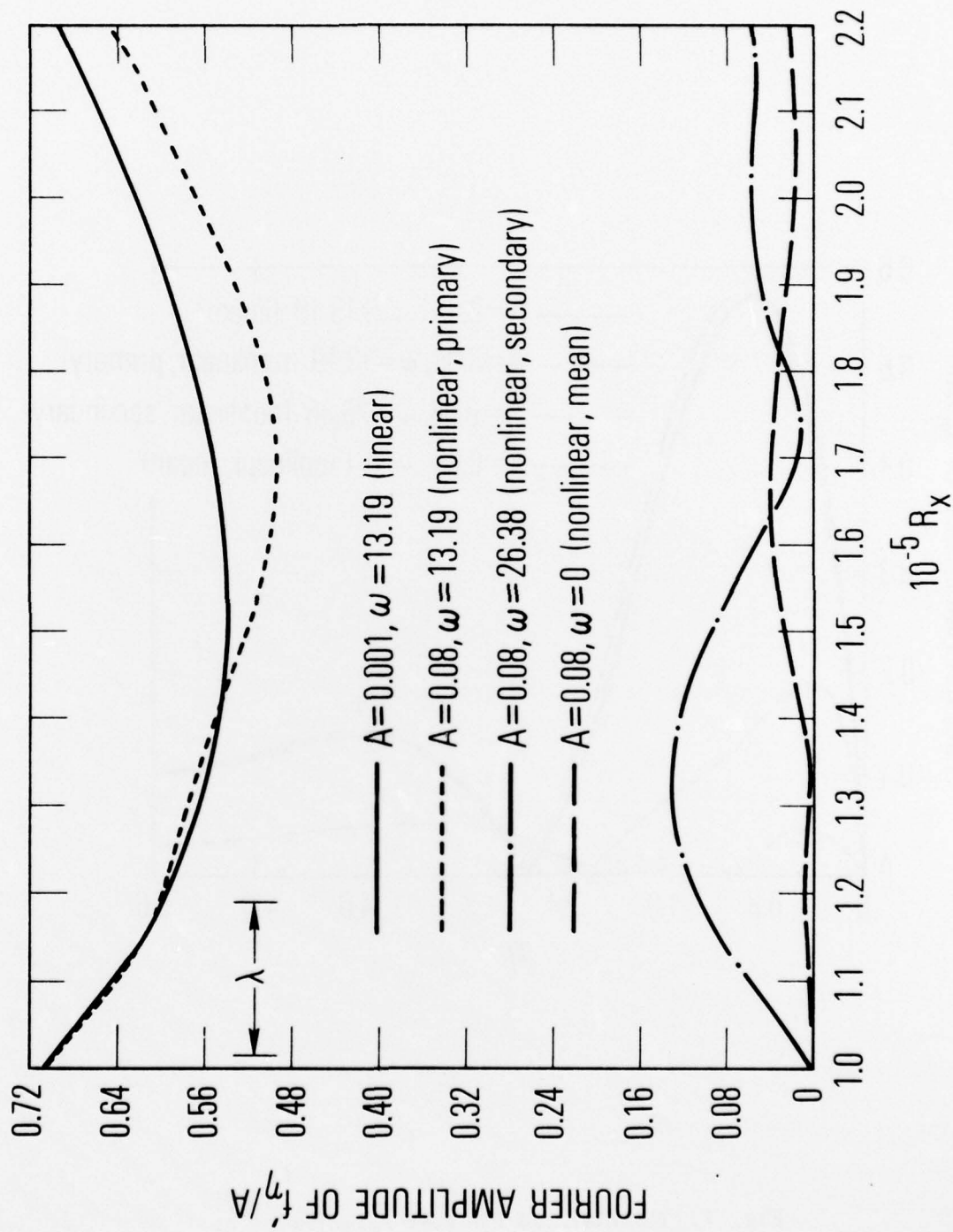Fig. 5. Fourier Transformed Velocity at $\eta = 0.2$
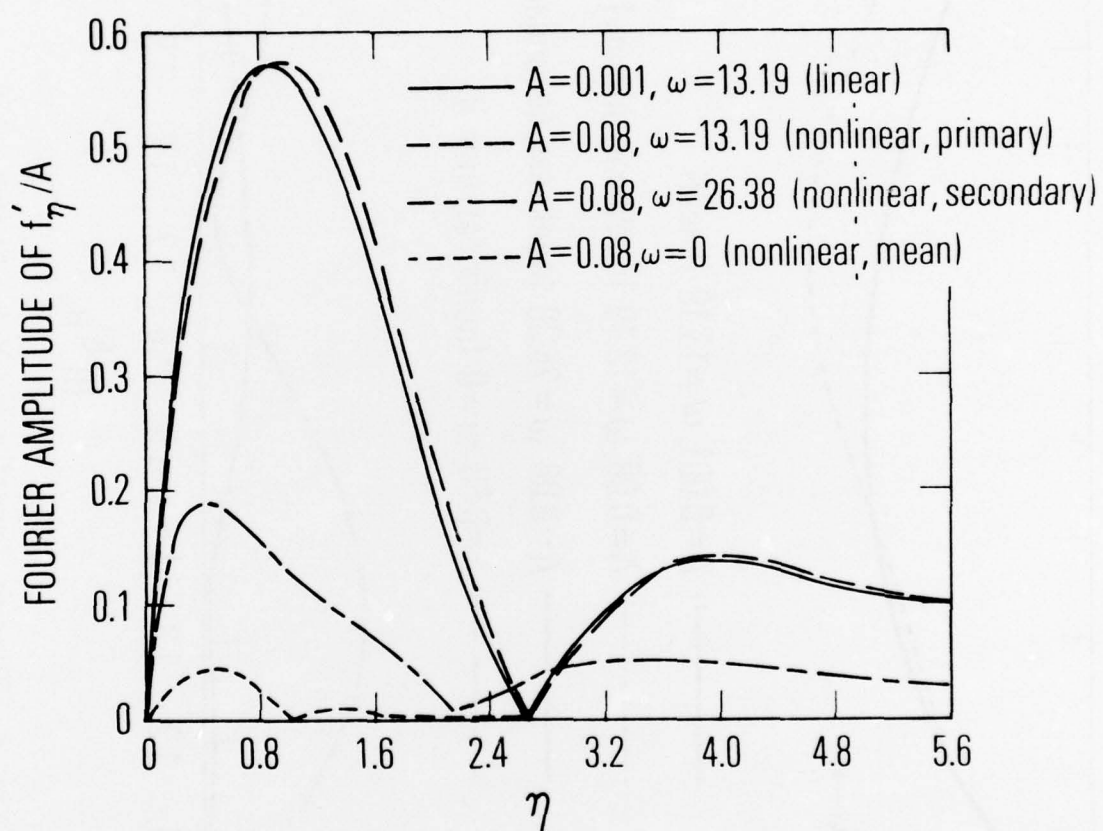
Fig. 6. Fourier Transformed Velocity at $\eta = 1.0$

Fig. 7. Normalized Fourier Amplitudes at
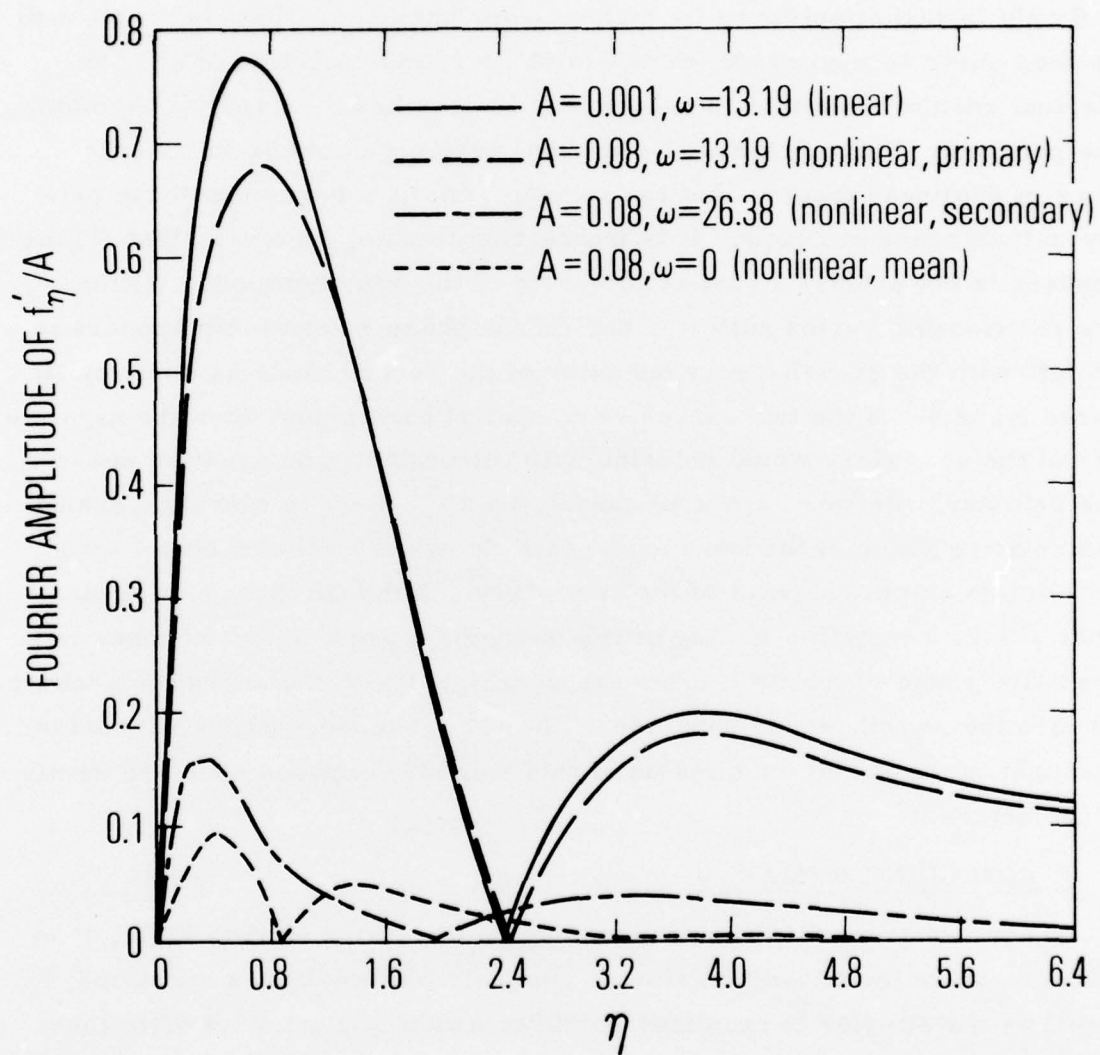$R_x = 1.3 \times 10^5$

Fig. 8. Normalized Fourier Amplitudes at
$R_x = 2.2 \times 10^5$

It is also of interest to consider the phase relationship between the primary and secondary modes. The sine of the phase angle for both modes is plotted versus R_x in Figure 9. The phase angle has been designated $\alpha x + \theta$ only to call attention to its higher order behavior. That is, if α (or θ) for either curve is a constant, then θ (or α) is a weak function of x. The numerical results show that the secondary is very nearly a spatial harmonic of the primary. This agrees with the usual assumption made in analytic studies of nonlinear theory, that the second mode is a harmonic of the primary in both space and time. It is interesting to note, however, that (1) the secondary is not exactly a spatial harmonic of the primary mode, (2) the phase relationship varies with R_x, and (3) the phase relationship appears to correlate with the growth-decay behavior of the second mode as depicted in Figures 5 and 6. If the two curves were spatial harmonics, then the negative peaks of the secondary would coincide with the positive and negative peaks of the primary. Between 1.6×10^5 and 1.8×10^5, there is clearly a change in the relative phase of the two modes; this change is well correlated with the minimum amplitude point of the secondary. Although this point needs further study, a tentative finding of this numerical work is that changes in the relative phase of the two modes are correlated with the energy interchange and hence the growth/decay behavior of the second mode. (Work carried out subsequent to the initial submission of this report[17] expands upon and verifies this conjecture.)

5. CONCLUDING REMARKS

There are four main results or conclusions of this work. First, it is possible to solve the two-dimensional, unsteady Navier-Stokes equations (as well as the simpler parabolized vorticity equations) using an orthogonal function expansion (spectral method) in both space dimensions with nontrivial boundary conditions. The most difficult problems arose with regard to the

[17] Murdock, J.W. and T.D. Taylor, "Numerical Investigation of Nonlinear Wave Interaction in a Two-Dimensional Boundary Layer," AGARD Symposium on Laminar Turbulent Transition, Copenhagen, Denmark. 2-4 May 1977.

$\omega = 13.19$ ------ $\omega = 26.38$

$\sin(\alpha x + \theta)$

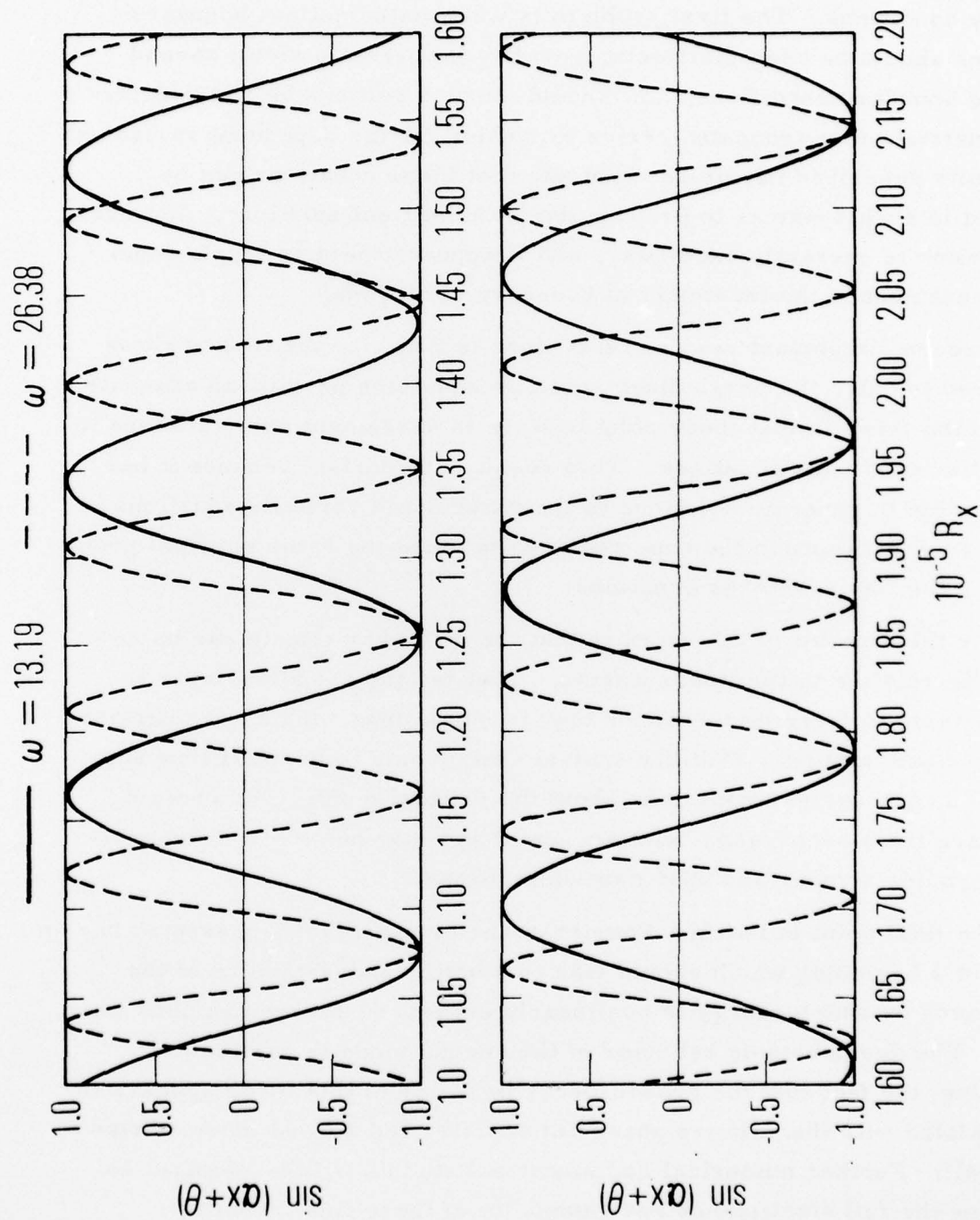$\sin(\alpha x + \theta)$

$10^{-5} R_x$

Fig. 9. Sine of the Phase Angle of the Primary and Secondary Wave at $\eta = 0.2$

boundary conditions. The first problem is what mathematical boundary conditions should be used (particularly on the downstream side); second, given the boundary conditions, how should these conditions be implemented to be consistent with truncated series expansion for the dependent variables? The results described herein demonstrate that these equations can be answered in such a way as to produce useful numerical solutions. However, further work is currently under way, and it appears there is ample room for improvement in the treatment of boundary conditions.

A second important result of this work is that, for the type of flows considered to date, the parabolized vorticity equations provide an adequate model of the flow, in that these solutions are in agreement with solutions to the full Navier-Stokes equations. This result is important because it has been possible to generate solutions to the parabolized vorticity equations in as little as one-twentieth the time required to solve the same physical problem using the Navier-Stokes equations.

The third result of this work is that the nonlinear effects can be destabilizing relative to the linear effects. That is, the boundary layer is more unstable to large disturbances than to small ones. This is important since previous nonlinear stability analyses apply only to parallel flow and, in addition, are series expansions about the critical point. The present results are for a nonparallel boundary layer and may be obtained for arbitrary Reynolds number and upstream disturbance.

The final point is that the Fourier-transformed results presented herein represent a beginning which should lead to a better understanding of the mechanisms by which energy is nonlinearly exchanged between various wave modes. The nonmonotonic behavior of the second mode is particularly interesting; the fact that the growth/decay behavior of this mode appears to be correlated with the relative phases of the first and second mode is also a new result. Further numerical and analytical studies will be required to determine the full significance and generality of these final results.

REFERENCES

1. Gaster, M., "On the Effects of Boundary-Layer Growth on the Flow-Stability," J. Fluid Mech., Vol. 66, 1974, pp. 465-480.

2. Stewartson, K., "Some Aspects of Nonlinear Stability Theory," Polish Academy of Sciences, Vol. 7, 1975, pp. 101-128.

3. DeSanto, D. F. and H. B. Keller, "Numerical Studies of Transition from Laminar to Turbulent Flow over a Flat Plate," J. Soc. Indust. Appl. Math., Vol. 10, 1962, pp. 569-595.

4. Fasel, H., "Numerical Solution of the Unsteady Navier-Stokes Equations for the Investigation of Laminar Boundary Layer Stability," Proceedings of the Fourth International Conference on Numerical Methods in Fluid Dynamics, Springer-Verlag, Berlin, 1974. pp. 151-160.

5. Fasel, H., "Investigation of the Stability of Boundary Layers by a Finite-Difference Model of the Navier-Stokes Equations," J. Fluid Mech., Vol. 78, 1976, pp. 355-383.

6. Orszag, S. A., "Turbulence and Transition: A Progress Report," Proceedings of the Fifth International Conference on Numerical Methods in Fluid Dynamics, Springer-Verlag, Berlin, 1976, pp. 32-51.

7. Roache, P. J., Computational Fluid Dynamics, Hermosa Publishers, Albuquerque, New Mexico, 1972, pp. 154-161.

8. Goldstein, S., Lectures on Fluid Mechanics, Interscience, London, 1960, pp. 136-144.

9. Orszag, S. A. and M. Israeli, "Numerical Simulation of Viscous Incompressible Flows," Annual Rev. of Fluid Mech., Vol. 6, 1974, pp. 281-318.

10. Fox, L. and I. B. Parker, Chebyshev Polynomials in Numerical Analysis, Oxford University Press, London, 1968.

11. Lanczos, C., Tables of Chebyshev Polynomials, U.S. Department of Commerce, National Bureau of Standards, Applied Mathematics Series 9, Washington, D.C., 1952, pp. v-xxvii.

REFERENCES (Continued)

12. Cooley, J.W., P.A.W. Lewis, and P.D. Welch, "The Fast Fourier Transform Algorithm: Programming Considerations in the Calculation of Sine, Cosine and Laplace Transforms," J. Sound Vib., Vol. 12, 1970, pp. 315-337.

13. Orszag, S.A., "Numerical Simulation of Incompressible Flows Within Simple Boundaries. I. Galerkin (Spectral) Representations," Studies in Applied Math, Vol. L, 1976, pp. 293-327.

14. Israeli, M., "A Fast Implicit Numerical Method for Time Dependent Viscous Flows," Studies in Applied Math, Vol. LIX, 1970, pp. 327-349.

15. Israeli, M., "On the Evaluation of Iteration Parameters for the Boundary Vorticity," Studies in Applied Math, Vol. LI, 1972, pp. 67-71.

16. Lynch, R.E., J.R. Rice, and D.H. Thomas, "Direct Solution of Partial Difference Equations by Tensor Product Methods," Numerische Mathematik, Vol. 6, 1974, pp. 185-199.

17. Murdock, J.W. and T.D. Taylor, "Numerical Investigation of Nonlinear Wave Interaction in a Two-Dimensional Boundary Layer," AGARD Symposium on Laminar Turbulent Transition, Copenhagen, Denmark, 2-4 May 1977.